

Chapter 6

SATELLITE MEASUREMENTS FOR OPERATIONAL OCEAN MODELS

Ian Robinson

Southampton Oceanography Centre, University of Southampton, U.K.

Abstract: This chapter outlines the character of ocean measurements from satellites in relation to their use by operational ocean forecasting models. Following a generic introduction to the field of satellite oceanography, it outlines the basic remote sensing methodology for measuring some key variables used by models; sea surface height from altimetry, ocean colour, sea surface temperature and ocean waves. It then presents the approach adopted by an international programme for combining sea surface temperature data from many sources, as an example of the issues involved in effectively preparing satellite data for ingestion into models. It concludes with comments on the actions needed to achieve the integration of satellite and *in situ* data with ocean models in an operational system.

Key words: Satellite oceanography, altimetry, sea surface height, ocean colour, sea-surface temperature, ocean waves, GODAE, ocean models, GHRSSST.

1. Introduction

The purpose of this chapter is to outline the basic characteristics of ocean measurements obtained from Earth-orbiting satellites. It introduces the reader to the subject within the particular context of considering how satellite ocean data can be used operationally to support model based ocean observing and forecasting systems.

After 25 years in which a number of methodologies have been developed to measure different aspects of the surface ocean, there are now many satellite-derived ocean data products available. A new generation of oceanographers takes it almost for granted that they can find global datasets of sea surface temperature and ocean colour, or detailed images of a particular ocean area, readily accessible through the Internet. The impact of the global revolution in telecommunication, capable of transporting

megabytes of data around the globe in seconds, has expanded the vision of ocean scientists so that we are now contemplating the creation of ocean forecasting systems for operational applications. We envisage systems in which observational data from sensors on satellites and *in situ* platforms are fed in near-real time into numerical models which describe the state of the ocean. Just as meteorologists look to numerical models, supplied by the global meteorological observations network, to give them the most complete and reliable view of what is happening in the atmosphere, so we expect that in future the output of ocean forecasting models will greatly improve the daily knowledge of the state of the ocean needed by operational users to manage the marine environment and to save life at sea.

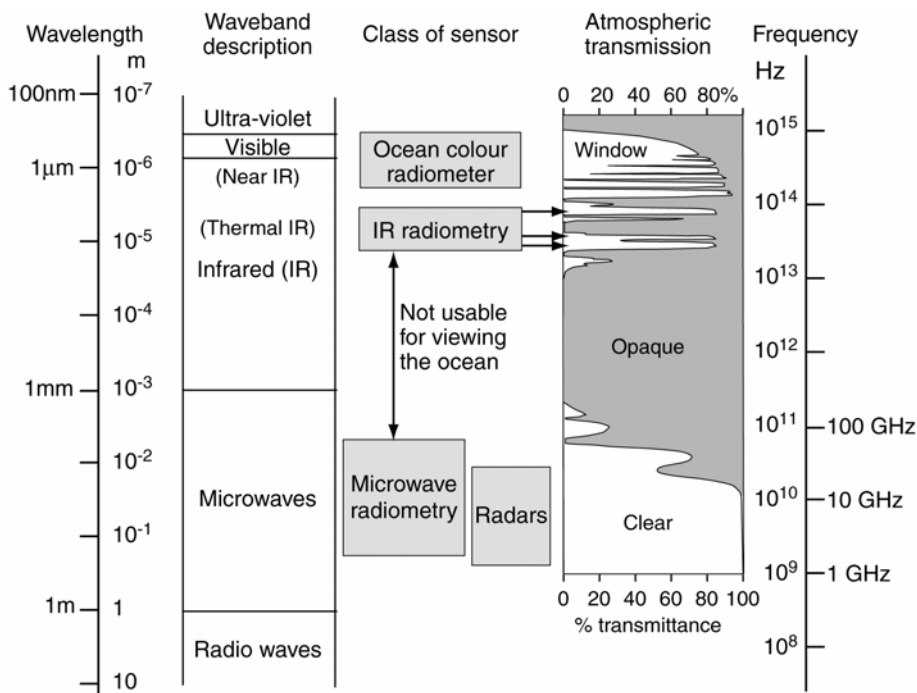


Figure 1. The electromagnetic spectrum, showing atmospheric transmission and the parts used by different remote sensing methods.

Computer models depend on observational data to ensure that they represent the true state of the ocean as closely as possible. It is therefore essential that the observational data fed into ocean forecasting systems are themselves as accurate as possible. It is also important that the limitations and inaccuracies inherent in remote sensing methods are understood and properly accounted for when such data are assimilated into models, or used to initialise, force or validate the models. If use is made of datasets broadcast on the Internet, the user should find out what processes have been

performed on them, and whether they are suitable for the purpose. For example some data products may contain “cosmetic” filling of values in locations where there would otherwise be gaps due to cloud cover or other obstructions to the remote sensing process. Ideally only true observations, and not the artefacts of data processing, should be presented to the numerical model.

This chapter is therefore written for those engaged in developing operational oceanography systems, to give them a basic background in the methods of ocean remote sensing so that they can appreciate what issues to consider as they evaluate the quality of satellite data. It is split into three main sections. The first is a generic overview of the subject. The second introduces the basic remote sensing methodology for some of the key variables used by models. These are sea surface height from altimetry, ocean colour, sea surface temperature (SST) and ocean waves. The third main section uses the example of SST to explore how measurements retrieved from several different sensor systems and supplied by different agencies can be most effectively combined to serve the needs of ocean forecasting models. It presents the methods adopted by an international programme established by the Global Ocean Data Assimilation Experiment (GODAE) for this purpose.

2. Methods of satellite oceanography: An outline

2.1 Using the electromagnetic spectrum

All satellite remote sensing sensors use electromagnetic (e.m.) radiation to view the sea. The ability of particular sensors to measure certain properties of the ocean and how well they can view through the atmosphere or penetrate clouds depends critically on which part of the e.m. spectrum they use. Figure 1 shows the section of the electromagnetic spectrum that is of relevance to remote sensing, and the four broad classes of sensors that are used. The diagram also shows how the transmittance of the atmosphere varies with e.m. wavelength, which accounts for why sensors are found only in certain wavebands. A much fuller account is given by Robinson (2004).

For much of the e.m. spectrum the atmosphere is opaque and therefore unusable for remote sensing of the ocean. However in a number of “window” regions of the spectrum most of the radiation is transmitted although it may be attenuated to some extent. These windows provide the opportunities for ocean remote sensing.

One of the windows extends from the visible part of the spectrum (between 400 nm and 700 nm, used by the human eye) into the near infrared (NIR). This is used by “ocean colour” radiometers that observe sunlight reflected from the ocean, both from the surface and from within the upper

few metres of the water column, with the potential to carry information about those contents of sea water such as chlorophyll, dissolved organic material and suspended particulates that affect the colour of sea water. Solar radiation in the near infra-red (wavelengths above 700 nm) is rapidly absorbed in water and so is not reflected out. Consequently any NIR radiation detected by an ocean-viewing radiometer is evidence of atmospheric scattering or surface reflection, and can be used to correct the visible part of the spectrum for those effects.

There are several narrow windows at wavelengths between about 3.5 μm and 13 μm that are exploited by infrared (IR) radiometers. This is the thermal IR part of the spectrum in which most of the detected radiation has been emitted by surfaces according to their temperature. In ocean remote sensing it is used for measuring sea surface temperature (SST). Like ocean colour, the presence of cloud interrupts the use of this waveband.

At much longer wavelengths, greater than a few millimetres, the atmosphere becomes almost completely transparent. This is referred to as the microwave spectral region. Between those parts of the microwave frequency spectrum allocated by international regulation to radio and TV broadcasts, telecommunications, mobile telephony and so on, a few narrow bands are reserved for remote sensing, within the broad regions indicated in Figure 1. Different bands are used for microwave radiometry and radars. Microwave radiometers are passive sensors, simply measuring the naturally ambient radiation that is emitted by the ocean, atmosphere and land surfaces. Radars are active microwave devices which emit pulses and measure the echoes from the sea surface, in order to gain information about some aspect of the surface.

There is a variety of different types of radar, which can be distinguished by the direction in which they point, the length and modulation of the emitted microwave pulse, and the way the echo from the sea surface is analysed. Radars can be classed as either viewing straight down at the nadir point below the platform, or viewing obliquely to encounter the surface at an incidence angle between 15° and 60°. The nadir sensors measure the surface height or slope and are called altimeters. Those viewing obliquely measure the surface roughness at length scales comparable to the radar wavelength. This is represented by a property of the radar interaction with the material and the geometry of the surface called σ_0 , the normalised radar backscatter cross-section.

2.2 Generic processing tasks for analysing ocean remote sensing data

Figure 2 illustrates schematically what is involved in measuring properties of the ocean using a sensor that is typically hundreds or thousands of kilometres from the sea surface. An electromagnetic signal of a particular

kind leaves the sea carrying information about one of the primary observable quantities which are the *colour*, the *temperature*, the *roughness* and the *height* of the sea. This must pass through the atmosphere where it may be changed, and where noise may be added to it, before it is received by the sensor which detects particular properties of the radiation and converts each measurement into a digital signal to be coded and sent to the ground. The sensor geometry restricts each individual observation to a particular instantaneous field of view (IFOV). In order to convert the numbers received at the ground station into scientific measurements of useful precision and quantifiable accuracy, the remote sensing process represented in the left side of Figure 2 must be inverted digitally using the knowledge and information identified on the right side.

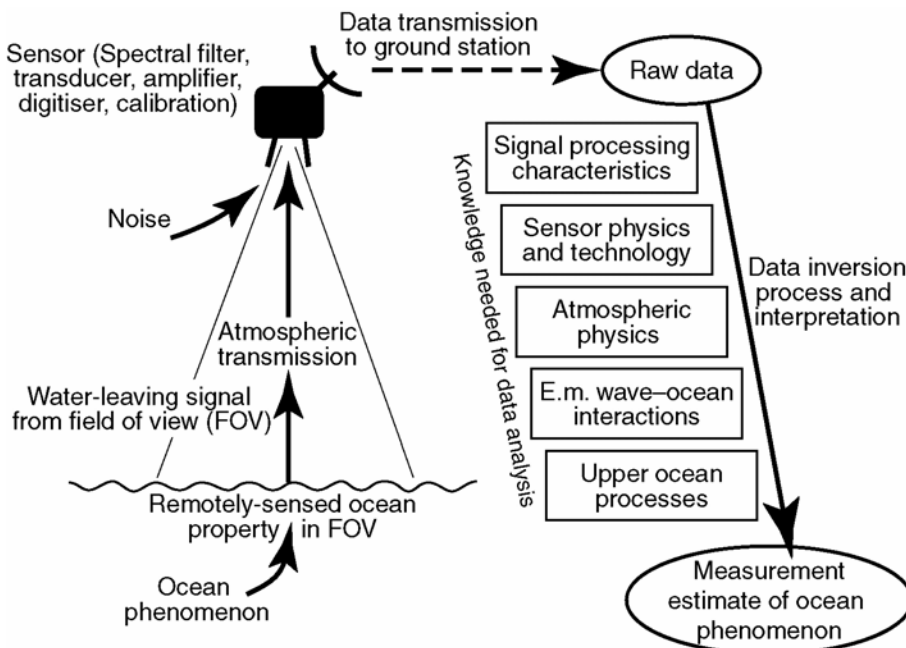


Figure 2. Schematic of information flow in ocean remote sensing.

Although there are just four observable quantities¹ and these are measured only at the very surface of the sea, apart from colour, it is surprising how much information about other properties or ocean processes can be retrieved from these four variables. Many phenomena in the upper ocean have sufficient influence on one or more of the primary measurable quantities to generate a “surface signature” in remotely sensed data and images. Some of these are obvious and predictable, such as the influence of

¹ The capacity to measure a fifth quantity from space, salinity, waits to be demonstrated by the European Space Agency’s SMOS sensor.

a near-surface phytoplankton bloom on the colour of the sea. Other signatures took many scientists by surprise when they were first discovered in the satellite images. For example internal waves, a dynamical phenomenon centred tens of metres below the sea surface, can sometimes be revealed in exquisite spatial detail in the images of synthetic aperture radar (SAR), because of their surface roughness signature.

In order to extract quantitative information about an ocean phenomenon from satellite data, we need to understand the physical processes in the upper ocean that control its surface signature in one of the primary detectable variables. Several of the derived properties, such as chlorophyll concentration retrieved from colour sensors, surface wind speed from scatterometers, wave height from altimetry, wave spectra from SARs and salinity from microwave radiometry are now being used, or proposed, for ingestion into ocean models. Figure 3 summarises the different classes and types of sensors, the primary variables which they detect, and the way in which they can supply inputs to ocean models.

For many of the applications to ocean models noted above, it is possible to use ocean data products already produced by the agencies responsible for the sensors, without the user having to engage themselves in any of the processing tasks. Nonetheless, it is important for users to be aware of the calibrations, corrections, analyses and resampling that are applied to data products before they are distributed, since these processes have impacts on the quality, accuracy and timeliness of the data. Figure 4 summarises them, and also indicates what is meant by the different “levels” of data products that may be available. Robinson (2004) provides a detailed explanation of what is involved in each of these processes.

2.3 The sampling constraints imposed by satellite orbits

The use of Earth orbiting satellites as platforms for ocean-viewing sensors offers a number of unique advantages such as the opportunity to achieve wide synoptic coverage at fine spatial detail, and repeated regular sampling to produce time series several years long. However, these benefits are won at the cost of being tied to the unavoidable constraints imposed by the physical laws of satellite orbital dynamics.

There are just two basic types of orbit useful for ocean remote sensing, geostationary and near-polar. The geostationary orbit, at a height of about 36000 km, has a period of one sidereal day (~23.93 hr). Placed over the Equator, the satellite flies West to East at the same rate as the Earth’s rotation, so it always remains fixed relative to the ground, allowing it to sample at any frequency. Being fixed it can view only that part of the world within its horizon, which is a circle of about 7000 km radius centred on the Equator at the longitude of the satellite. Its great height also makes it difficult for sensors to achieve fine spatial resolution.

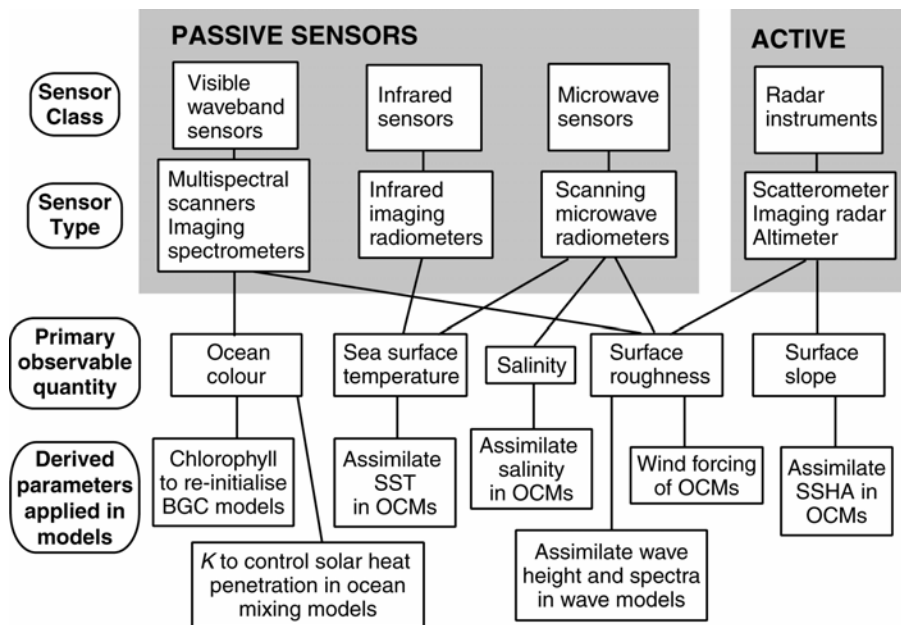


Figure 3. Summary of the different classes and types of ocean sensors carried on satellites, indicating the primary quantity which each sensor type measures and ways in which the derived parameters are used in numerical models including ocean circulation models (OCM) and biogeochemical models (BGC).

In a near-polar orbit the satellite flies at a much lower altitude, typically between about 700 km and 1350 km, for which the orbital period is about 100 min. It thus completes between 14 and 15 orbits a day, during which the Earth rotates once, so the satellite marks out a ground track crossing about 14 times northeast to southwest (descending tracks) and the same number of southeast to northwest ascending tracks. The tracks are distributed evenly around the globe, with successive orbits following a track about 24° of longitude to the east of the previous orbit. A wide-swath sensor that can scan across about 2800 km will thus view every part of the Earth twice a day, once from an ascending and once from a descending orbit. An even wider swath permits more samples per day as swaths from successive orbits overlap at the Equator, while at higher latitudes overlapping occurs for much narrower swaths. However, the global coverage is won at the price of a much reduced sampling frequency compared to the geostationary orbit.

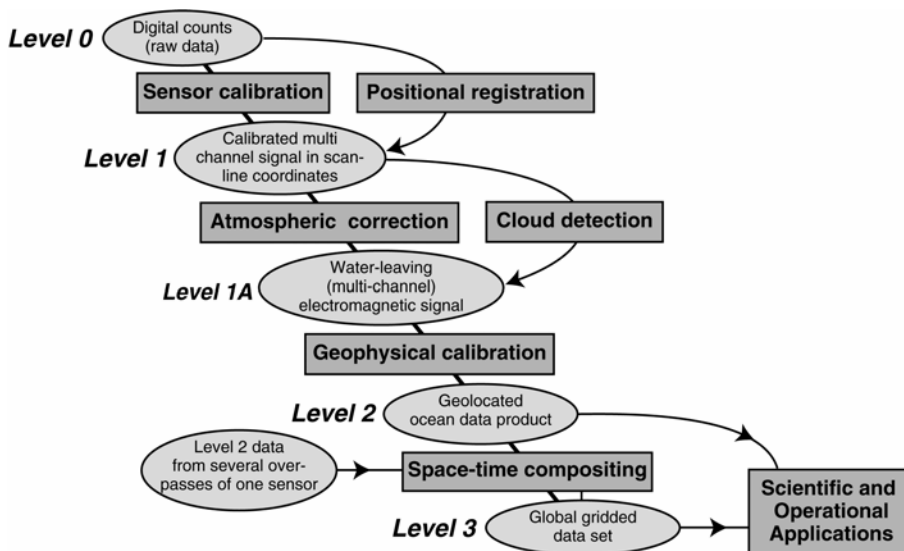


Figure 4. Outline of data processing tasks to convert raw satellite data into ocean products suitable for operational applications, showing the different “levels” of processed data which are produced at each stage.

For much narrower swaths (normally associated with fine resolution imaging sensors) or for non-scanning instruments such as the altimeter that sample only along the ground track, the time between successive views of the same location depends on the precise way in which the orbit repeats itself. If the orbit repeat period is just a few days then the sensor revisit interval will be the same, but in this case a narrow swath sensor will miss many parts of the Earth surface altogether. Global coverage by a sensor whose swath is about 200 km would take about 15 days to accomplish. A non-scanning sensor builds up a sampling pattern that progressively fills the gaps left by previous orbits until one orbit repeat cycle is completed when the tracks repeat. For scanning and non-scanning sensor alike, there is evidently a well defined trade-off between spatial and temporal sampling capability, which is discussed in more detail by Robinson (2004). It is important to appreciate these fundamental constraints when designing an ocean observing system for operational purposes. For example, the only way to ensure that even a wide swath sensor can sample every six hours is to fly sensors on two satellites. Ideally a combination of spatial and temporal resolution should be selected in order that important phenomena can be adequately sampled. If mesoscale eddies are to be monitored then the spacing between orbit tracks should not be wider than their variability length scale, nor should the repeat cycle be longer than the characteristic lifetime of an eddy. Otherwise some eddies may be missed altogether.

Most satellites in a low, near-polar orbit are sun-synchronous. By choosing an inclination that is slightly greater than 90° (i.e. their path does

not quite reach the poles) the orbit plane is constrained to precess at a rate of once per year relative to the stars. This locks the overpasses to the position of the sun and means that every orbit always crosses the Equator at the same local solar time. For most ocean observing sensors this is very convenient, since it ensures that the longitudinal position of the sun does not change from one sample to the next, even though the solar latitude inevitably changes with the annual cycle. However, for altimetry the sun-synchronous orbit is to be avoided since it aliases the solar semidiurnal tidal constituent.

2.4 Strengths and weaknesses of ocean remote sensing

The global, spatially detailed and regularly repeated views of the oceans that have been obtained from satellites for more than a decade have made them an important part of the design of operational ocean monitoring systems. It is therefore worth summarising the benefits that satellite ocean data bring as well as noting their limitations.

The importance of satellite data to oceanography can be highlighted by the way they have opened up the study of global ocean phenomena. We can now ask questions about large scale processes which could not properly be addressed scientifically until remote sensing methods allowed us to make observations of ocean scale phenomena which test and stretch the theoretical models. A good example of this is the study of oceanic Rossby waves (Challenor *et al.*, 2004). To some extent 21st Century Oceanography has become dependent on satellite observations. All branches of ocean science now expect to use satellite image data and interest in the subject is no longer limited only to specialist “satellite oceanographers”. Another powerful impact has come from the immediacy of satellite data. Observations from all around the world are now being made available within hours, minutes in some cases, of their acquisition by the sensor, and this has reinforced their importance for use in operational ocean monitoring and forecasting

At the same time we must not overlook the fundamental limitations of satellite ocean remote sensing methods. They can observe only some of the ocean’s properties and variables. They measure the ocean only at or near the surface although it can be argued that, of all the parts of the ocean, the surface is the most critical place to be able to measure. Most critically, ocean measurements may be corrupted by the atmosphere and some methods cannot see through clouds at all. Moreover, measurements cannot be made “to order” but only when the satellite is in the right place. Finally it must not be overlooked that all measurements from satellites require calibration and / or validation using *in situ* data. While it might be carelessly thought that satellites can remove the need for measurements at sea, the reverse is in fact the case. The full benefit of the wider and higher perspective achieved from satellite data will only be realised when combined with an integrated array of *in situ* sensors interfacing with operational ocean models.

3. Some satellite measurements used for operational models

3.1 Sea surface height anomaly from altimeters

3.1.1 The principles of altimetry over the ocean

A satellite altimeter is a nadir-viewing radar which emits regular pulses and records the travel time, the magnitude and the shape of each return signal after reflection from the earth's surface. The travel time is the essential altimetric measurement, leading to a determination of the ocean surface topography at length scales longer than about 100 km. Ocean surface topography contains information about ocean dynamical and geophysical phenomena. If the travel time can be measured to a precision of 6×10^{-11} s then, knowing the speed of light, the distance can be calculated to a resolution of 1 cm. Corrections have to be made to allow for the changed speed of light through the ionosphere and the atmosphere, and for delays associated with reflection from a rough sea surface (Chelton *et al.*, 2001). It is generally agreed that for these corrections to approach the target accuracy of 1 cm a dual frequency altimeter must be used (to determine the ionospheric refraction), and a three channel microwave radiometer is needed to sound the water vapour in the atmosphere.

The altimeter is not an imaging sensor. Viewing only the nadir point below the satellite, it simply records measurements of distance between the satellite and the sea surface along the ground track. As discussed in 2.2, the spatial and temporal sampling characteristics therefore depend entirely on the exact orbit repeat cycle of the satellite. This was chosen to be about 10 days for the TOPEX/Poseidon (T/P) and Jason altimeters which fly on platforms dedicated to the altimetric mission, although for other altimeters it has ranged between 3 days, 17 days and 35 days. The longer the revisit interval the finer the spatial sampling grid. Typically, ocean topography data are interpolated onto a geographical grid and composited over the period of an exact repeat cycle, to produce "images" which are comparable with global SST or ocean chlorophyll composite images although produced in a completely different way.

By itself, knowing the distance, R_{alt} between the ocean surface and a satellite is of limited value. Figure 5 shows what else needs to be defined or measured for this to yield an oceanographically useful property. First of all, when the height of the satellite, H_{sat} , is known relative to a reference level, then the height, h , of the sea above the reference level can be determined. The reference level is a regular ellipsoid-shaped surface defined within a frame of reference fixed in the rotating earth. It is chosen to match approximately the shape of the earth at sea level, and provides a convenient datum from which to measure all other heights.

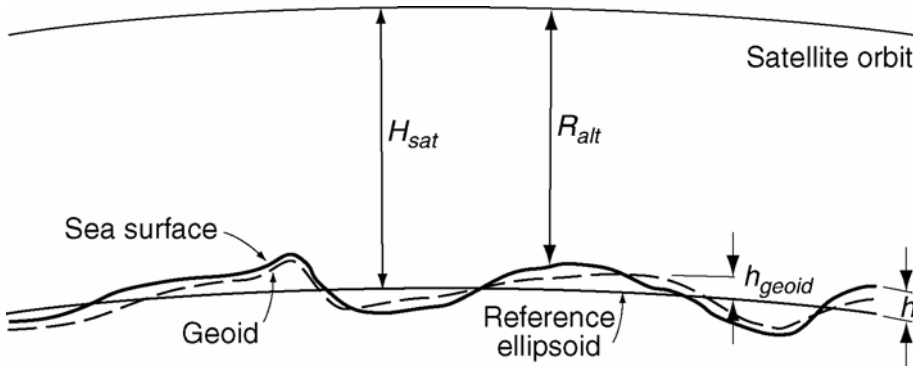


Figure 5. The relationship between different distance quantities used in altimetry

Several physical factors contribute to h , which is called the ocean surface topography. The first is the distribution of gravity over the earth, as represented by the geoid, at height h_{geoid} above the reference ellipsoid in Figure 5. The geoid is the equipotential surface, at mean sea level, of the effective gravitational field of the earth which incorporates earth-rotation forces and the gravitation of the solid earth, the ocean itself and the atmosphere. By definition it is normal to the local effective gravity force, and if the ocean were everywhere in stationary equilibrium relative to the

earth, its surface would define the geoid.

Another factor which contributes to h is h_{tide} , the instantaneous tidal displacement of the sea surface relative to its tidally averaged mean position, including the contribution of the Earth tide. A third is the local response, h_{atm} , of the ocean to the atmospheric pressure distribution over the ocean, approximated by the inverse barometer effect in which an increased pressure of 1 mbar lowers sea level by 1 cm. The remaining factor is the displacement of the sea surface associated with the motion of the sea, called the ocean dynamic topography h_{dyn} . Thus:

$$h = h_{dyn} + h_{geoid} + h_{tide} + h_{atm} \quad (1)$$

The dynamic topography is the property which is of most relevance for ocean modelling since it contains information about the ocean circulation. Rearranging (1) and substituting $h = H_{sat} - R_{alt}$ yields:

$$h_{dyn} = H_{sat} - R_{alt} - h_{geoid} - h_{tide} - h_{atm} \quad (2)$$

The accuracy and precision of the estimated ocean dynamic height depends not only on the altimetric measurement itself but also on the other four terms in (2). For dedicated altimetry missions flying at a height of

about 1340 km where atmospheric drag is minimal, the height of the satellite in orbit, H_{sat} , can now be predicted to a precision of 2 cm (Tapley *et al.*, 1994) using a combination of laser and microwave tracking devices and an orbit model using precise gravity fields. The tidal contribution has been evaluated along the repeat orbit track by tidal analysis of the altimeter record spanning several years (Le Provost, 2001). Because the tidal frequencies are very precisely known the response to each constituent can be evaluated to an accuracy better than 2 cm in the open ocean, even though the sampling interval of about 10 days is longer than most of the tidal periods. This is only possible when the precise period of the repeat cycle is chosen to avoid any serious aliasing with one of the major tidal constituents. For this reason a sun-synchronous orbit, which aliases the S_2 (solar semidiurnal) tidal signal, should not be used. Over shelf seas where tides are very high and can vary rapidly over short distances it is not so easy to remove the tides and so the estimate of dynamic height is less accurate. The atmospheric pressure correction is based on the output of atmospheric circulation models.

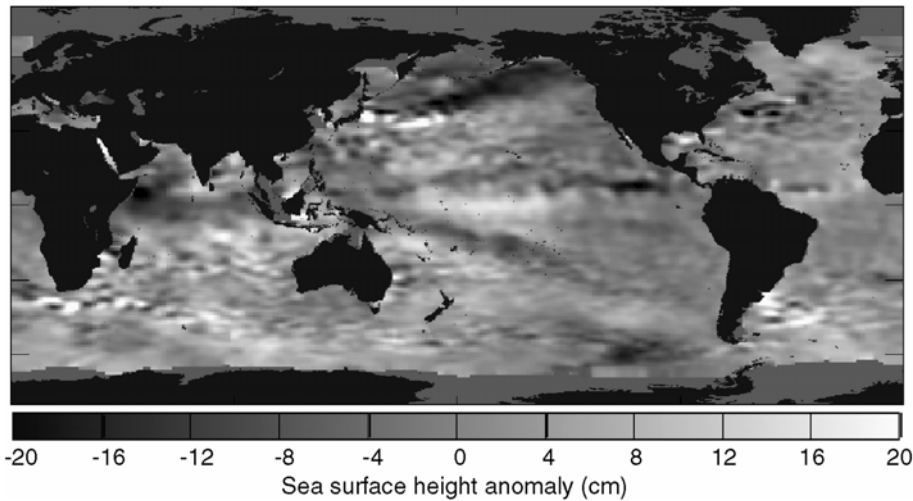


Figure 6. The spatially averaged SSHA field from TOPEX/Poseidon for 31 Dec, 2001. (Image generated with data obtained from JPL at podaac.jpl.nasa.gov/poet)

3.1.2 Evaluating sea surface height anomaly

At present, the geoid is not known independently and so oceanographers must be content with measuring the combined $h_{dyn} + h_{geoid}$. Of these, the typical magnitude of the spatial variability of h_{geoid} is measured in tens of metres, about ten times greater than that of h_{dyn} , which is why until recently the time-mean ocean topography from altimeters provided geophysicists with the best measure of the geoid. However, h_{geoid} does not vary with time,

at least not sufficiently to be detected by an altimeter over tens of years, whereas the time-variable part of h_{dyn} is comparable in magnitude with the mean component, of order metres over a few months. Therefore the time variable part of h_{dyn} , called the sea-surface height anomaly, SSHA, can be separated from the measured $h_{dyn} + h_{geoid}$ by simply subtracting the time mean over many orbit cycles. To enable a time-mean to be produced, the orbit track must be precisely repeated to within a kilometre and the data must be accumulated from several years of a ten-day cycle. For this reason it is essential to fly a new altimeter in precisely the same orbit as its predecessor so that the mean surface topography of the earlier mission can be used straight away. Then SSHA can be calculated from the first orbit cycle of the new altimeter, without having to wait another few years to build up a new mean topography for a different orbit track.

It is important to remember that the SSHA, which is widely used and assimilated into ocean models, does not contain any information about the dynamic height of the ocean associated with the mean circulation. Thus in Figure 6, which is an example of the SSHA from T/P observed during a ten-day period in December 2001, the dominant features are mesoscale eddies. The dynamic topography signatures of the strong ocean currents are not seen at all, apart from the fact that the eddy-like activity is strongest where the major currents tend to meander.

Altimeter	Agency	Dates	Height	Orbit	Accuracy
TOPEX/ Poseidon	NASA/ CNES	1992- present	1336 km	9.92 day repeat non- sun-synchronous	2-3 cm
Poseidon-2 on Jason-1	NASA/ CNES	2001- present	1336 km	9.92 day repeat non- sun-synchronous	~2 cm
Radar altimeter (RA) on ERS-1	ESA	1991- 2000	780 km	3 & 35 day repeat sun-synchronous	~5-6 cm
RA on ERS-2	ESA	1995- 2003	780 km	35 day repeat sun- synchronous	~5-6 cm
RA2 on Envisat	ESA	2002- present	800 km	35 day repeat sun- synchronous	3 cm
Geosat	U.S. Navy	1986-89	800 km	17.05 day repeat sun-synchronous	10 cm reanalysis
Gesosat Follow-on	U.S. Navy	2000- present	880 km	17.05 day repeat sun-synchronous	~10 cm

Table 1. Recent and current series of satellite altimeters

There are presently three families of altimeters in operation, as listed in Table 1 with the details of their altitude, orbit repeat and the approximate accuracy (root mean square) of an averaged SSHA product. The T/P–Jason family is a joint French/U.S.A. dedicated altimetry mission in a high non-sun-synchronous orbit. In contrast the Geosat and ERS series are on lower sun-synchronous platforms for which the orbit prediction accuracy would be,

on their own, much poorer. However, because these satellites cross over each other's orbits tracks it is possible, over an extended time span, to significantly improve their orbit definitions by cross-referencing to the better known T/P or Jason orbits. The accuracy quoted for the SSHA applies only after this procedure has been performed, and would otherwise be much worse for the ERS and Geosat families. The specification of errors for an altimeter must be handled with care because the error magnitude relates very much to the time and space scale over which it is being averaged. The lower error attached to larger-scale / longer-period averaging must be offset against the lesser utility of the averaged SSHA field, especially in the context of operational oceanography.

3.1.3 Variable currents from sea surface height anomaly

To determine an estimate of the time-variable part of ocean surface currents the geostrophic equations are used:

$$\begin{aligned}fv &= g \frac{\partial h_{SSHA}}{\partial x} \\fu &= -g \frac{\partial h_{SSHA}}{\partial y}\end{aligned}\tag{3}$$

where (u, v) are the East and North components of the geostrophic velocity, f is the Coriolis parameter, g is the acceleration due to gravity and x and y are distances in the East and North direction respectively.

From a single overpass, only the component of current in a direction across the altimeter track can be determined, but where ascending and descending tracks cross each other the full vector velocity can be estimated. Because Eq. (3) assumes geostrophic balance, if there is any ageostrophic surface displacement it will lead to errors in (u, v) . However, ageostrophic currents should not persist for longer than half a pendulum day ($1/f$) before adjusting to geostrophy. Thus the spatially and temporally averaged SSHA maps produced from all the tracks acquired during a single repeat cycle (10, 17 or 35 days depending on the altimeter) should represent a good approximation to a geostrophic surface that can be inverted to produce the surface geostrophic currents.

This raises an interesting question when SSHA is to be assimilated into an ocean circulation model. Most models which use altimeter data presently assimilate the global or regional field from a whole orbit cycle, and perhaps combine the data from the different altimeter families shown in Table 1. But this means some of the data may be many days old by the time they can be ingested into the model and therefore of less utility in improving the accuracy of operational nowcasts or forecasts. Alternatively models can in

principle assimilate the SSHA along track records within a few hours of acquisition. While the data errors will be greater, the input will be timely. If the model variables are properly matched to the altimeter data it may even be possible to use the ageostrophic information contained in the non-averaged along track record.

Close to the Equator the SSHA cannot be interpreted directly in terms of surface currents since here f is very small and the geostrophic Eq. (3) cannot be applied.

In the relatively near future it is hoped that the lack of knowledge about the Geoid can be remedied. What is needed is a means of measuring h_{geoid} without using altimetry, and this is provided by the measurement of the gravity field above the Earth from satellites. Both the presently operating Gravity Recovery And Climate Experiment (GRACE) and the Gravity and Ocean Circulation Explorer (GOCE) mission which is due for launch by 2007 measure elements of the gravity field from which it is possible to recreate the sea-level Geoid. At the required accuracy of about 1 cm the GRACE can achieve this only at a length scale longer than at least 1000 km, but it is expected that the GOCE can do so once-for-all down to a length scale of about 100 km. This will allow the steady state ocean currents to be derived from archived altimetric data and greatly improve the capacity to utilise altimetric data in near-real time.

3.1.4 The impact of altimeters on oceanography

Despite the present limitations of altimetry to measuring just the time-variable part of surface currents in the open ocean only, this achievement by itself has made a tremendous difference to Oceanography in the 21st Century. It has opened up the whole approach to operational ocean forecasting based on numerical modelling, since without the capacity of altimetry to monitor the mesoscale turbulence of the ocean at time scales of days to weeks there would be little hope of ensuring that ocean models remain consistent with the real ocean. The ability to measure changes in the absolute height of the sea to an accuracy of 2-3 cm (a measurement uncertainty of just 2 parts in 10^8) is technologically quite breathtaking, yet instrument engineers and data analysts do not believe the limits to further improvement have been reached. The measurement of the geoid independently of altimetry will liberate more information from the altimeter record within a few years from now. Meanwhile, there remains the challenge to develop methods of assimilating SSHA into ocean models which fully recognizes the character of the altimeter data and maximises the utilisation of the available information.

3.2 Ocean colour

The light measured by an ocean colour sensor pointing towards the sea comes originally from the sun. Photons of light on their path from the sun to the sensor have encounters with the medium, such as reflection at the sea surface and scattering in the atmosphere or ocean, while some photons are absorbed and never reach the the sensor. To the extent that the outcome of these encounters are spectrally sensitive, the resulting colour (spectral distribution) of the light reaching the sensor contains information about some aspects of the sea and the atmosphere. Figure 7 summarises the factors which affect the colour. Direct solar reflection, sun glitter, tends to dominate all other signals when it is present and so it is avoided as far as possible by the choice of orbit geometry and overpass time, and in some cases by deliberately tilting the sensor away from the specular reflection of the sun over that part of the orbit where it would otherwise be a problem. The rougher the surface the wider becomes the sea area affected by sun glitter but the magnitude of the reflected radiance in any particular direction is reduced.

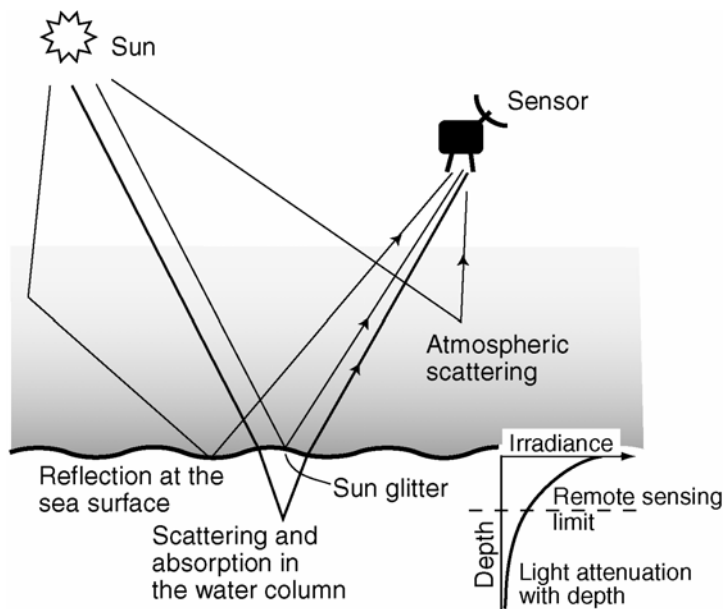


Figure 7. Interaction of sunlight with the atmosphere and ocean

3.2.1 Atmospheric correction

For the satellite oceanographer, the “signal” consists of the light reflected from below the sea surface since its colour can be interpreted in relation to the water content. All the other interactions cause additions or alterations to

the signal, producing noise which requires correction. The greatest contribution comes from light scattered by the atmosphere into the field of view of the sensor, which may make up over 90% of the measured radiance, including skylight reflected by the sea surface into the sensor. The atmospheric correction procedure must account for this in order to estimate the water leaving radiance for each of the spectral bands recorded by the sensor.

Scattering by the air gas molecules themselves can be directly calculated for each pixel in the field of view of an imaging sensor, but scattering by larger particles of aerosols such as water vapour or dust particles cannot be calculated because their distribution in the atmosphere is unknown and impossible to predict. Instead this part of the atmospheric correction uses the radiance measured in two spectral bands from the near infra-red part of the spectrum. Because the sea absorbs almost all incident solar near-infrared radiation, any measured at the top of the atmosphere must have been scattered by the atmosphere. This is then used to estimate how much aerosol scattering has occurred in the visible channels where the water leaving radiance is not zero, and so the correction is accomplished.

3.2.2 Estimating water content from its colour

When the atmospheric correction has been successfully applied to satellite ocean colour data, the result is an estimate of the water-leaving radiance in each spectral channel in the visible waveband, normalised to reduce dependence on the sun's elevation and the viewing incidence angle. Effectively the normalised water leaving radiance should represent what a sensor would measure if looking straight down from an orbit that takes it just above the sea surface at the bottom of the atmosphere. This is what our eyes would detect as the colour and brightness of the sea, ignoring any light reflected from the surface. The primary challenge of ocean colour remote sensing is to derive quantitative estimates of the type and concentration of those materials in the water which affect its apparent colour.

Photons of visible wavelength e.m energy from the sun that enter the sea will eventually interact with molecules of something in the sea. The outcome will be either that the photon is scattered, in which case it may change its direction with a chance of leaving the sea and contributing to what the sensor sees, or it will be absorbed. The probability of scattering or absorption depends on the wavelength of the light and the material which it encounters. The molecules within sea water tend to preferentially scatter shorter wavelengths of light (the blue part of the spectrum) and preferentially absorb longer wavelengths (the red end). This is why pure sea water with little other content appears blue.

The pigment chlorophyll-*a* which is found in phytoplankton has a strong and fairly broad absorption peak centred at 440 nm in the blue, but not in the

green. Therefore, as the chlorophyll concentration increases, more blue light is absorbed while the green light continues to be scattered and so from above the sea water looks greener. This is the basis for many of the quantitative estimates of sea water content derived from satellite ocean colour data. The typical form of an algorithm to estimate the concentration of chlorophyll (C) or phytoplankton biomass is:

$$C = A(R_{550}/R_{490})^B \quad (4)$$

where A and B are empirically derived coefficients and R_λ is the remote-sensing reflectance (radiance coming out of the sea towards the sensor, normalised by ingoing irradiance) over a spectral waveband of the sensor centred at wavelength λ . When using the wavelengths indicated in Eq. (4) this is described as the green / blue ratio. In the open sea it is possible to estimate C to an accuracy of about 30% by this means. Most algorithms presently in use are somewhat more complex than Eq. (4) but still closely related to it. If the sample data from which the coefficients A and B etc. are derived is representative of many different open sea situations then such algorithms can be applied widely in many locations.

Other substances which interact with the light and so change the apparent colour of the sea are suspended particulate material (SPM) that has a fairly neutral effect on colour except in the case of highly coloured suspended sediments, and coloured dissolved organic material (CDOM, sometimes called "yellow substance") which absorbs strongly towards the blue end of the spectrum. Both of these affect the light along with the chlorophyll "greening" effect when there is a phytoplankton population. However because the chlorophyll, CDOM and SPM all co-vary within a phytoplankton population the green-blue ratio effect dominates the colour and each of these materials can be quantified by an algorithm such as Eq. (4), as long as phytoplankton are the only major substance other than the sea water itself which is affecting the colour. Such conditions are described as being Case 1 waters, and it is here that the ocean colour algorithms work fairly well to retrieve estimates of C from satellite data.

However, if there is SPM or CDOM present from a source other than the local phytoplankton population, for example from river run-off or resuspended bottom sediments, then we can no longer expect any simple relationship between the concentrations of these and C . In this situation the green-blue ratio algorithms do not perform very well, if at all, and it becomes much harder to retrieve useful quantities from ocean colour data using universal algorithms. These situations are described as Case 2 conditions. Unfortunately it is not easy to distinguish between Case 1 and Case 2 waters from the satellite data alone. This can result in very degraded accuracy with errors of 100% if the chlorophyll algorithms are applied in Case 2 waters. It is prudent to classify all shallow sea areas as Case 2,

particularly where there is riverine and coastal discharge or strong tidal currents stirring up bottom sediments, unless *in situ* observations confirm that Case 1 conditions apply.

Another useful measurement that can be derived from the ocean colour is the optical diffuse attenuation coefficient, K , usually defined at a particular wavelength such as 490 nm (i.e. K_{490}). This is also inversely correlated with the blue-green ratio because the less the attenuation coefficient, the deeper the light penetrates before it is scattered back out, the more of the longer wavelengths are absorbed, and the bluer the water appears. The algorithms for K are similar in form to (4) and are less sensitive to whether Case 1 or Case 2 conditions are found.

3.2.3 Ocean colour sensors and products

Although visible wavelength radiometers were among the very first Earth observing sensors flown in the 1970s the development of ocean colour sensors is less mature than that of other methods of satellite oceanography. After the Coastal Zone Color Scanner (CZCS) proved the concept of measuring chlorophyll from space in 1978-1986, there was a long pause until the Ocean Colour and Thermal Sensor (OCTS) was launched in 1996, followed by the Sea-viewing Wide Field-of-view Sensor (SeaWiFS) in 1997, which has provided the first reliable, long-term fully operational delivery of ocean colour data products. Since then two Moderate resolution imaging spectrometers (MODIS), the Medium resolution imaging spectrometer (MERIS) and the Global Imager (GLI) have been launched (see Table 2). All fly in low (~800 km) sun-synchronous polar orbits, providing a resolution at nadir of about 1.1 km and almost complete Earth coverage in 2 days. Other colour sensors have also been flown by individual countries offering less comprehensive coverage and poorer data availability than those listed.

Sensor	Agency	Dates	No. of visible channels	No. of near-IR channels
CZCS	NASA	1978-86	4	-
OCTS	NASDA	1996-97	6	2
SeaWiFS	NASA	1997-present	6	2
MODIS/Terra	NASA	2000-2004	7	2
MERIS	ESA	2002-present	8	3
MODIS/Aqua	NASA	2002-present	7	2
GLI	NASDA	2002-2003	12	3

Table 2. Details of the major satellite ocean colour sensors

All of the sensors listed in Table 2 are supported by a calibration and validation programme and their data are worked up by the responsible agency into derived oceanographic products at level 2 and in some cases

level 3. In all cases some measure of C is produced and an estimate of K is derived globally. These are generally reliable products and C approaches the target accuracy of 30% in open sea Case 1 waters. However great care must be taken when using the products over coastal and shelf sea (possibly Case 2) waters where the potentially large errors could give misleading information. Some of the agencies attempt to provide a number of other products such as SPM and CDOM but these are yet to be proven.

3.2.4 Using satellite ocean colour data in ocean models

The use of ocean colour derived data products in ocean models is in its infancy. The long and successful deployment of SeaWiFS has given some confidence that ocean colour sensors are capable of supplying data for operational applications. However the disappointing loss of two excellent sensors (OCTS and GLI) through spacecraft failure, and the difficulties with calibrating the MODIS/Terra products, have slowed down any moves in this direction. It is to be hoped that, when MODIS/Aqua and MERIS are fully proven and delivering data products routinely within a few hours of acquisition, they will establish an even better operational supply of data than SeaWiFS which is approaching the end of its operational life.

There are two main ways in which ocean colour data are likely to be used operationally. The first is to use measurements of C to improve the modelling of phytoplankton biomass in numerical ocean models which contain a biogeochemical, phytoplankton or carbon cycle component. The uncertainties associated with modelling biological populations are such that improvements can be gained by assimilating or otherwise ingesting measurements of C even when their accuracy is no better than 30%. So far the most promising approach has been to use the satellite observations to identify when and where a phytoplankton bloom emerges, since it is particularly difficult for a model to trigger the initiation of a bloom. Satellite data are used to update or re-initialise a model with the newly emerged bloom conditions. The problem of cloud cover and the uncertain accuracy make the data less useful to the model for the stage when the modelled bloom has peaked and then gradually decays.

The other main use of colour data is in providing K for physical models which need to know how far solar radiation penetrates into the sea. Thus models of mixed layer development and the occurrence of a diurnal thermocline, which are sensitive to K , can benefit from being regularly updated with information about how K is distributed and varies in space and time.

Another factor which still needs more investigation is the relationship between the near-surface measurements of C which satellites provide and the distribution of C with depth. Because phytoplankton need light to thrive, then it is reasonable to suppose that most will be detected by ocean colour

sensors. However, as indicated in Figure 7 a visible waveband radiometer will “see” only down to the level where the irradiance is about 1/3 of its surface value. The satellite measurements are unlikely to record accurately, if at all, any phytoplankton below this level, such as those contributing to the deep chlorophyll maximum found at the base of a mixed layer after nutrients have been used up from the mixed layer. Similarly if a second, low-light, species develops below the main bloom the satellite will not be able to detect them.

There is undoubtedly a large amount of valuable information for ocean models to be found in the ocean colour data products from satellites. However considerably more research is needed to learn how best to inject that information into the models. A particularly enticing prize is to combine the satellite measurements with ocean carbon cycle models to be able to estimate with some confidence the rates of primary production occurring in the sea. Allied to this is the potential for improving our knowledge of how pCO₂ (representing the amount of CO₂ dissolved in the surface water) is distributed, leading to better estimates of air-sea fluxes of CO₂. Finally we should not overlook the much simpler application of using ocean colour as a tracer of mesoscale eddies. There is a need to develop techniques to assimilate this information so that eddy-resolving ocean circulation models are guided to present eddies in the right place at the right time.

3.3 Sea surface temperature

3.3.1 Diverse methods for measuring sea surface temperature

Sea surface temperature (SST) can be measured in a variety of ways, using sensors on both satellites and *in situ* platforms (Robinson & Donlon, 2003). Sampling from *in situ* platforms can generally be performed at high frequency whereas most satellite methods are severely restricted by orbit constraints to long sampling intervals of several hours or more. On the other hand remote sensors are capable of wide synoptic spatial coverage at fine spatial detail down to 1 km resolution when unobstructed by clouds, while all the *in situ* methods sample very sparsely, and may miss some regions altogether. Table 3 lists the different classes of satellite-based methods and the typical absolute accuracy of measurements which they can achieve. Relative accuracy (that is the smallest temperature difference that can be detected confidently within a given image from a single overpass) may be somewhat better than the absolute value quoted.

Instrument	Spatial coverage and nadir resolution	Time sampling	Accuracy
Polar orbiting IR radiometer (e.g. AVHRR)	Global; 1.1 km,	12 hr; cloud-limited	0.3 - 0.5 K
Polar orbiting dual view IR radiometer (e.g. AATSR)	Global; 1 km	Twice in 2-4 days, cloud-limited	0.1 - 0.3 K
Polar-orbiting microwave radiometer (e.g. AMSR-E)	Global; 25 - 50 km	12 hr - 2 days	0.3 - 0.5 K
Geostationary orbit IR sensor (e.g. SEVIRI on Meteosat S.G.)	50°S - 50°N; 2-5 km	30 min, cloud-limited	0.3 - 0.5 K

Table 3. Classes and characteristics of satellite temperature sensors

Space methods for measuring SST are differentiated both by the part of the electromagnetic spectrum used and by the orbit of the platform from which the Earth is viewed. Sensors placed on geostationary satellites such as Meteosat and GOES are capable of regular and frequent (15-30 min) sampling throughout every 24 hr period but are limited in spatial coverage by the horizon at 36,000 km altitude. Because they are so far above the Earth a very fine angular resolution is required to achieve useful spatial resolution at the sea surface. This presently rules out the use of microwave radiometers and so all SST sensors in geostationary orbit use the infrared. This makes them vulnerable to cloud cover, but they are able to take advantage of any clear skies which may develop at any time of the day or night.

The sensor type used most for global SST monitoring is the infrared scanner on polar orbiting satellites. The NOAA Advanced Very High Resolution Radiometer (AVHRR) series has been routinely flown since 1978, with normally two satellites operational at any time in a sun synchronous orbit providing morning and afternoon overpasses plus two night-time overpasses (Kidwell, 1991). Since 1991 a series of along-track scanning radiometers (the ATSR class) has been flown on ESA polar platforms. Using the same infra-red wavebands as the AVHRR, these sensors have a unique design allowing them to observe the same part of the sea surface twice, once looking almost straight down and the other viewing obliquely. This dual view capability significantly improves the atmospheric correction.

The third approach is to use microwave radiometers in polar orbit, operating at 6 or 10 GHz. Although not so sensitive or easy to calibrate as infrared instruments, and having much coarser spatial resolution, microwave radiometers have the advantage over infrared of being able to view through clouds and are insensitive to the presence of atmospheric aerosol.

3.3.2 Satellite infrared sensors

An infrared sensor records the radiance detected at the top of the atmosphere in specific wavebands, λ_n . The individual measurements in each channel, n , can be expressed as an equivalent black body brightness temperature, T_{bn} , that is the temperature required for a black body with 100% emissivity to emit the measured radiance. At a particular wavelength, black body emission is defined by the Planck equation:

$$L(\lambda, T) = \frac{C_1}{\pi \lambda^5 [\exp(C_2/\lambda T) - 1]} \quad (5)$$

where L is the spectral radiance, per unit bandwidth centred at λ , leaving unit surface area of the black body, per unit solid angle ($\text{W m}^{-2} \text{m}^{-1} \text{sr}^{-1}$), λ is the wavelength (m), T is the temperature (K) of the black body, $C_1 = 3.74 \times 10^{-16} \text{ W m}^2$, and $C_2 = 1.44 \times 10^{-2} \text{ m K}$. This must be integrated with respect to wavelength over the measured waveband and convoluted with the spectral sensitivity of the sensor in order to represent the radiance intercepted by a particular spectral channel.

To obtain T_{bn} from the digital signal S_n recorded by the sensor for waveband n requires direct calibration of the sensor using two on-board blackbody targets of known temperatures which straddle the range of ocean surface temperatures being observed. This is the method adopted by the ATSR class of sensor, whereas the AVHRR uses the simpler but less accurate alternative of a single on-board black body with a view of cold space serving as an alternative to the second black body.

Ideally we wish to measure the radiance leaving the water surface, which is determined by the skin temperature of the sea, T_s , and by the emissivity of seawater. In the thermal infrared this is greater than 0.98, but a small contribution to the satellite detected radiance comes from the reflected sky radiance, for which allowance must be made. Because of absorption by greenhouse gases T_{bn} is cooler than T_s by an amount which varies in time and place, mainly with the amount of atmospheric water vapour. It is the task of the atmospheric correction procedure to estimate T_s given top of atmosphere measurements of T_{bn} .

A well-established method of atmospheric correction is to make use of the differential attenuation in different wavebands. When viewing the same ground cell, different wavebands (i, j etc.) of the sensor would record the same temperature ($T_{bi} = T_{bj}$) if there were no atmospheric attenuation. The difference between the top of atmosphere brightness temperatures T_{bi} and T_{bj} is related to the amount of absorbing gases in the atmospheric path, so that algorithms of the form

$$T_s = aT_{bi} + b(T_{bi} - T_{bj}) + c \quad (6)$$

where a , b and c are coefficients to be determined, provide a good basis for atmospheric correction of the AVHRR (McClain *et al.*, 1985). During the day the "split-window" algorithm uses wavebands at 10.3-11.3 μm and 11.5-12.5 μm , while at night the 3.5-3.9 μm channel can also be used. This 3.7 μm channel is corrupted by reflected solar radiation in the daytime. A number of non-linear variants of this basic form have also been developed (Barton, 1995). The algorithm is also supposed to accommodate the non-blackness of the sea.

Common to each of these approaches for AVHRR is the requirement for the coefficients to be determined by a best fit between the satellite predictions and coincident observations of SST from a number of drifting buoys. The match between the buoys and satellites has a variance of more than 0.5 K, applicable only to the regions populated by the buoys (Podesta *et al.*, 1995). The same algorithms are assumed to apply to parts of the ocean where there are no buoys, although the validity of this assumption needs to be quantified. Regional algorithms matched to local data may achieve greater accuracy.

Although the instantaneous distribution of water vapour and aerosols in the atmosphere are not known, the radiation transfer physics of the atmosphere is well understood and can be modelled with some confidence in fine spectral detail. It is therefore possible to simulate T_b for a given combination of T_s , atmospheric profile and viewing angle for the spectral characteristics and viewing geometry of each channel of a particular sensor. This offers an alternative strategy for atmospheric correction in which an artificial dataset of matching T_s and T_{bi} , T_{bj} , etc. is created using a wide variety of typical atmospheric water vapour and temperature profiles. The coefficients for an equation of form similar to (6) are generated by a regression fit to the artificial dataset. The resulting algorithm should be applicable to all atmospheric circumstances similar to those included in the modelled dataset, leading to an estimate of the skin SST. It is independent of coincident *in situ* measurements, although they are needed for validation.

This was the approach adopted for the along track scanning radiometer (ATSR) flown on the ERS polar orbiting satellites (Edwards *et al.*, 1990). The ATSR scans conically to observe a forward view at about 60° incidence angle and a near-nadir view about two minutes later. Using the same three spectral channels as AVHRR for each of the views, it thus acquires six measures of brightness temperature. The different path lengths for forward and nadir views make for a more robust algorithm (Zavody *et al.*, 1995), less reliant on the spectral dependence of the atmospheric attenuation. The single-view approach was rendered inoperative when large volumes of volcanic dust were temporarily injected into the stratosphere by the eruption of Mt. Pinatubo in 1991 (Reynolds, 1993). Although the first ATSR

algorithms were also affected, a reworking of the semi-physical model by including the stratospheric aerosols in the radiation model led to algorithms which cope well with the volcanic problem (Merchant *et al.* 1999). This approach should also be robust in situations such as those where dust from the Sahara is lifted into the troposphere over the Atlantic.

The atmospheric correction algorithms produce maps of SST at fine resolution (about 1.1 km) for each overpass. However, the atmospheric correction methods cannot retrieve SST when cloud wholly or partly obstructs the field of view. Therefore at this stage cloud must be detected using a variety of tests (e.g., Saunders and Kriebel, 1988), so that only cloud-free pixels are retained for oceanographic applications, such as assimilation into models. The most difficult cloud contamination to identify is that by sub-pixel size clouds, thin cirrus or sea fog where only small deviations of temperature occur. Failure to detect cloud leads to underestimation of the SST and can produce cool biases of order 0.5 K. Thus confidence in the cloud detection procedure is just as important as atmospheric correction for achieving accurate SST. Where uncertainty remains in cloud detection, this should be flagged in the error estimate fields attached to SST products. Cloud detection is generally more successful during daytime, when visible and near-IR image data can be used, than at night.

The SSTs measured in individual overpasses are incorporated into global composite datasets by averaging all individual pixel contributions to each larger cell over a period of a few days. The larger cells are defined by longitude and latitude on a grid with spacing typically 1/2 or 1/6 degree (about 50km or 16 km at the equator). The multi-channel sea surface temperature (MCSST) (Walton *et al.*, 1998) was the standard global composite product derived from AVHRR, until superseded by the Pathfinder SST (Vasquez *et al.*, 1998). This is a re-processing of the archived pixel-level AVHRR data with algorithms incorporating the best knowledge of sensor calibration drift and making full use of the available drifting buoy dataset (Kilpatrick *et al.*, 2001). It also makes more use of night-time data than previous analyses, and aims for long term consistency. Reynolds and Smith (1994) developed an OI-SST archive that is an optimal interpolation of both *in situ* and satellite data, and should therefore provide more climatological continuity with pre-satellite SST records before 1980. The global composite product from ATSR is the ASST (Murray, 1995) which is being re-processed using the more robust atmospheric algorithms (Merchant *et al.*, 1999).

3.3.3 Microwave radiometers on satellites

Microwave radiometers detect the brightness temperature of microwave radiation which, like the infrared, depends on the temperature of the emitting

surface. Their great benefit is that their view is not impeded by cloud and very little attenuation occurs in the atmosphere, although water present as large liquid drops in precipitation does attenuate the signal. However, the emissivity, ϵ , of the sea surface in the microwave part of the spectrum is less than 0.5. ϵ also depends on factors such as the temperature, the salinity and the viewing incidence angle. This in turn means the brightness temperature is also a function of the mean square slope and hence of the sea surface roughness and wind speed. While this complicates the retrieval of SST from microwave radiometry compared with infra-red methods, the corollary is that microwave sensors can be used to measure the surface roughness, rainfall or even salinity as well as SST.

It is possible to distinguish between the different contributions to the brightness temperature of SST, surface roughness and salinity, as well as to identify atmospheric contamination by liquid water, because each factor differentially affects different microwave frequencies. For example SST strongly affects wavebands between 6 and 11 GHz whereas the effects of salinity are found only at frequencies below about 3 GHz. Surface roughness effects influence frequencies at 10 GHz and above, and are also polarisation specific. Thus a multi-frequency and multi-polarisation radiometer can, in principle, be used to measure SST, surface wind and precipitation (see chapter 8 of Robinson (2004)). Each of these has potential for use in ocean models, and coincident measurement of SST and winds has potentially useful applications in the estimation of air-sea fluxes.

Despite a long series of microwave sensors flown for atmospheric remote sensing, serious consideration of microwave measurements of SST from space started only when a microwave radiometer having a 10.7 GHz channel was flown on the Japanese-US Tropical Rainfall Mapping Mission. Called the TRMM microwave imager (TMI) it has a spatial resolution of 0.5° (about 50 km) and because it over-samples it is capable of mapping mesoscale eddies quite effectively using a grid scale of 25 km. It lacks the preferred SST waveband of 6.6 GHz, but its 10.7 GHz channel is sensitive to SST in tropical water temperatures (Donlon *et al.*, 2001), and its usefulness for measuring the thermal signatures of tropical instability waves has already been demonstrated by Chelton *et al.* (2000). It covers only latitudes lower than 40° .

In 2002 the Japanese Advanced Microwave Scanning Radiometer (AMSR-E) was launched into a near-polar orbit on the NASA Aqua satellite. This sensor includes a channel at 6.6 GHz, which is effective over the full range of sea temperatures, and has opened the way for routine, high quality, global mapping of SST by microwave radiometry. AMSR-E is now providing global cloud free SST to an accuracy of ~ 0.3 K derived from over-sampled 76 km resolution data. The composite daily, weekly and monthly SST products are supplied on a $1/4^\circ$ grid (Wentz and Meissner, 2000).

Microwave radiometers cannot be used within about 100 km of the coast because of the side-lobe contamination of microwave sources on land leaking into the antenna reception. This, with their low spatial resolution, severely limits their usefulness in coastal and shelf seas.

3.3.4 The character of the ocean surface thermal structure

The ocean modeller requiring measurements of SST, for assimilation or to validate the temperatures in the top layer of an ocean GCM, may conclude that their task is greatly simplified by the wide choice of different types of observations of SST now available from both *in situ* and satellite platforms. However, there is a pitfall for the unwary user of SST data, arising from the detailed character of the thermal structure in the top few metres of the ocean. Two distinct factors create near-surface vertical temperature gradients. Firstly on sunny calm days a diurnal thermocline tends to develop above which a top layer is found, a metre or so thick and up to about 1 K warmer than below (although exceptionally it can be several K warmer). At night the warm layer collapses. Secondly (and independently of the first effect) the top skin layer of the sea, a fraction of a millimetre thick, tends to be a few tenths of a Kelvin cooler than the water immediately below. Both these effects, and especially the first, may be horizontally variable, leading to spatial patchiness of SST.

Neither of these processes is normally represented in the physics of ocean models for which the topmost layer typically corresponds to the upper mixed layer assumed to be uniform above the seasonal thermocline. The different types of measurement of SST also sample at different levels of the near-surface thermal structure. In other words the definition of "SST" is different for the thermometer on a buoy's hull, for a sensor in a ship's cooling water intake, for an infrared radiometer, for a microwave radiometer, and for an ocean model. These differences are important when accuracies of a few tenths of a Kelvin are required. They may also vary considerably during the day so that a single daily measurement used may be aliased depending on the time in the diurnal cycle at which it is sampled. It is therefore necessary to harmonise SST data from different sources before they are introduced to an ocean model. This is one of the issues discussed in section 4 of this paper.

It is certainly worth taking the trouble to resolve these issues because SST observations can provide a very useful constraint on models. Surface ocean dynamical features often have thermal signatures. Major ocean currents are normally associated with thermal fronts. Ocean eddies are often visible in satellite SST images. Thus the assimilation of SST should in principle help to constrain the modelled evolution of mesoscale variability. In the case of coupled ocean-atmosphere models the interface temperature gains even more importance for constraining the model. In this case

particular care must be taken in defining which type of SST is needed, since the atmosphere is in contact with the skin temperature rather than the upper mixed layer temperature normally represented in the ocean model.

3.4 Ocean waves

The nowcasting and forecasting of ocean waves is an operational task which benefits many different users of the sea and is essential for the safety of mariners and for cost-effective navigation. Ocean wave forecasting models depend on good wind forecasts from numerical weather prediction models. Their performance can also be improved if good observations of wave data can be assimilated in a timely way. In situ measurements from wave buoys offer a means of testing and validating model predictions, but they are isolated and too few to make much impact if assimilated into a model. This requires the wide area coverage offered by satellites. Here we consider two ways in which ocean wave data potentially useful for models are measured from space.

3.4.1 Significant wave height measured by altimeters

When an altimeter measures the time for an emitted pulse to return, it tracks in detail the shape of the leading edge of the echo, from which it is possible to make a very good estimate of the significant wave height, $H_{1/3}$, within the pulse-limited footprint illuminated by the altimeter. For a perfectly flat calm surface the return echo has a very sharp edge. If there are large waves, several metres in height from trough to crest, then the return signal starts to rise earlier, as the first echoes are received from the crests, but takes longer to reach its maximum, when the first echoes are received from the wave troughs. The rising edge of the echo is modelled by a function in terms of the root mean square ocean wave height, so that by matching the observed shape to the model function it is easy to gain an estimate of $H_{1/3}$. This method has delivered robustly accurate measurements of $H_{1/3}$ for more than twenty years from different altimeters (Cotton & Carter, 1994) and comparison with buoys shows root mean square differences of only 0.3 m (Gower, 1996), which is the limit of the buoy accuracy.

It therefore provides an excellent source of information to be used in wave models. At present there are at least two altimeters in operation (see chapter 11 of Robinson (2004)), each crossing the Earth with 14-15 orbits per day. However, the altimeter footprint measures waves only along a 10 km wide swath along the satellite ground track. At the Equator the tracks of successive orbits are nearly 3000 km apart, and so in one day the available samples are quite sparse and it is possible to miss altogether local regions of high waves associated with a recent storm. Even with several altimeters in

complementary orbits it would be difficult to provide a reliable operational wave monitoring service based on observations alone. However, when the satellite data are assimilated into ocean wave forecasting models, their global coverage, their accuracy and their detailed resolution along the track ensure that they make a measurable improvement to the skill and reliability of wave forecasts. The major shortcoming of this type of wave measurement is that it contains no information about the wave direction.

3.4.2 Directional wave spectra from synthetic aperture radars

When a serious discrepancy is found between a wave model forecast and the measured wave height, it is desirable to know the directional properties of the waves so that incorrect wave energy sources in the model can be located and corrected. Directional wave spectra can be estimated using synthetic aperture radar (SAR). SARs view the sea surface obliquely and produce image maps of the backscattered microwave energy, at a spatial resolution of about 25m. The signal processing required to achieve this resolution is computationally intensive and can generate interesting artefacts, especially when the scattering surface is in motion (see Chapters 9 and 10 of Robinson (2004) for an introduction to SAR ocean imaging). The radar backscatter signal itself needs to be interpreted carefully. It represents a measure of the roughness of the sea surface at length scales similar to the radar wavelength, since a type of Bragg scattering mechanism is responsible for the radar echo from obliquely incident microwave pulses.

Swell waves appear on SAR images as approximately linear patches of bright and dark corresponding to regions where the backscatter is greater or less than the mean. There are three different mechanisms by which the swell waves modulate the short waves which determine the backscatter. A two-dimensional spectrum of the image amplitude is related to, but not the same as, the directional wave spectrum. The modulation transfer function which relates the ocean wave spectrum to the image spectrum depends on the swell wave frequency, their amplitude and their direction relative to the radar azimuth. The problem of accurately and reliably inverting image spectra to retrieve wave spectra has been a challenging field of research for two decades, although recent techniques which use the complex form of the SAR image (including the phase as well as the amplitude of the backscatter) look most promising (see Chapron *et al.* (2001) for a review of the subject). It is most important that users of SAR-derived wave spectra should understand that SAR can provide very little information about the shorter waves with period less than about 10 s, and this frequency cut-off is worse for waves propagating in a direction parallel to the satellite track.

The SARs of the European Space Agency can operate in a wave-mode in which small (5×10 km) imagettes are acquired every 200 km along track. Thus wave spectra can be sampled from across the global ocean every day.

As yet there is no operational ingestion of such data into wave models, but the improved spectra have raised new interest in doing so.

4. Preparing satellite SST for assimilation into models

4.1 Introduction

If SST data from space are to be used operationally as part of ocean observing systems and for creating a reliable, stable climate time series, there is a need to harmonise and inter-calibrate the SST products already being produced by several different agencies. Specifically for use in ocean forecasting models there is also a need to precondition the data to make them more immediately usable for assimilation into numerical models. This is true of most types of satellite data required by models although the processing tasks for preconditioning vary according to the parameter of interest. The blending and preparation of SST data differs from what has to be done for altimetric measurements of sea surface height anomaly or for parameters such as chlorophyll concentration derived from satellite ocean colour data. The rest of this chapter describes a new international initiative to perform the intermediate processing tasks needed to generate the best coherent products from complementary SST data delivered by several agencies. It serves as a specific illustration of the organisation and initiative that is desirable in order to enhance the usability in model assimilation of any observational parameter derived from several independent measurement programmes, particularly from satellites.

In 2001 the Global Ocean Data Assimilation Experiment (GODAE) prompted the creation of a working group which has developed into the GODAE high resolution sea surface temperature pilot project (GHRSS-PP). In the rest of this chapter, section 4.2 identifies the particular issues relevant to SST data and how these have been rationalised by the GHRSS-PP and formalised in the GHRSS Data Processing Model. Section 4.3 describes how a European project called Medspiration is about to start producing products conforming to the GHRSS-PP specifications. Section 4.4 concludes with a discussion of what can be learned more generally from the example of GHRSS-PP and Medspiration.

4.2 The challenge of assimilating SST data from many sources

4.2.1 Sampling and resolution capability of existing sensors

Section 3.3 noted that satellite sensors for measuring SST may be differentiated into four classes. The derivation of SST from the top-of-

atmosphere brightness temperatures recorded by the sensors identified in Table 3 is performed by a number of different agencies around the world, leading to a variety of SST data products. For example Table 4 lists the SST products available for European seas and the Atlantic Ocean. These are produced in near-real time, most are publicly available and can be served for use by operational models. Other SST sensors such as the infrared channels on MODIS have not been included because at present they are not processed within an operational timeframe.

Each product can be considered to be independent of the others. Even those derived from the same satellite source by different agencies are by no means identical because each agency has its own protocols regarding matters such as cloud detection, atmospheric correction algorithms, rules for compositing, confidence flags and error statistics. However there is at present little, if any, independent validation of most of the products, although ESA does have a formal AATSR product validation process.

The type of SST (see section 4.2.3) also differs according to the producer. Note for example that although AATSR and AVHRR measure radiation emitted from the sea-surface skin, the SST products from AVHRR are classified as either subskin or bulk, and from AATSR as skin, because of the different ways each producer calibrates the atmospheric correction.

The wide choice and apparent redundancy offered by the different sensors in Table 3 and SST data products in Table 4 prompts the question of which is the best to use for assimilation into ocean forecasting models. Because the measurement of global SST from space using polar orbiting infra-red sensors is a well established mature observational system, having acquired useful data for more than 20 years, it might seem reasonable to assume that it is ready to provide data for assimilation into ocean models.

However, stringent sampling requirements and a higher degree of accuracy are now demanded for applications in both climate monitoring and operational oceanography (Robinson and Cromwell, 2003). On closer inspection it seems increasingly difficult to meet these requirements using any one of the SST data products currently produced by several different agencies. No matter what improvements are made to sensor technology or atmospheric correction algorithms, the problem of cloud cover imposes unavoidable limits on the use of infra-red sensors, while microwave sensors which can penetrate the cloud are not capable of the required spatial resolution.

The most promising way to obtain the best SST data for input to models is by combining data from the different sensor types of Table 3 so that each product from Table 4 complements the others (Robinson and Donlon, 2003). Data from the AATSR provides the best absolute accuracy through that sensor's dual view, but coverage suffers from the narrow swath inherent in the viewing geometry and so it cannot achieve a revisit interval appropriate to operational applications at all latitudes. In contrast this is achieved by the

AVHRR with its less certain radiometric accuracy, although its wide swath and more frequent revisits can still not view the sea when cloud is present. This problem can be partly overcome in Equatorial regions by the use of geostationary sensors, which are available at all times of the day and night to see the sea whenever there are gaps in the cloud. Ultimately, however, the absence of IR observations caused by persistent cloud can be overcome only by the use of microwave sensors. Although their spatial resolution is very much inferior to that of infrared sensors, the recent improvement in their radiometric performance should enable them to contribute unique information to operational systems under persistently cloudy conditions.

Sensor name	Product name and resolution	Spatial coverage in specified time	Type of SST	Data provider
AATSR	ATS_NR_2P 1km	Global, pseudo 3 day repeat	Skin	ESA
AATSR	ATS-Meteo 10 arc min	Global, pseudo 3 day repeat	Skin	ESA
AVHRR NOAA16	GAC (1) 9km	Global, daily repeat	At 1m (2)	NAVOCEANO
AVHRR NOAA16	LAC (3) 2 km	Regional, at least daily repeat, day and night	At 1m (2)	NAVOCEANO
AVHRR NOAA16	NAR 2 km	Regional, at least daily repeat, day and night	Subskin	EUMESAT O&SI SAF
AVHRR NOAA17	GAC (1) 9km	Global, daily repeat	At 1m (2)	NAVOCEANO
AVHRR NOAA17	LAC (3) 2 km	Regional, at least daily repeat, day and night	At 1m (2)	NAVOCEANO
AVHRR NOAA17	NAR 2 km	Regional, at least daily repeat, day and night	Subskin	EUMESAT O&SI SAF
MSG SEVIRI	SEVIRI 0.1° lat./lon.	Regional, 3 hour repeat	Subskin	EUMETSAT O&SI SAF
GOES-East	GOES 4 km	Regional, 3 hour repeat	At 1m (2)	EUMETSAT O&SI SAF
GOES-East	GOES 6 km	Regional, 1/2 hour repeat	At 1m (2)	NAVOCEANO, PO.DAAC
TMI	0.25° lat./lon. grid	40°N - 40°S, daily	Subskin	REMSS
AMSR-E	0.25° lat./lon. grid	Global, daily repeat	Subskin	REMSS

1. GAC means the SST product is produced from the global area coverage, a reduced dataset stored on board and delivered once per orbit.
2. This expresses the definition of the product given by the data provider.
3. LAC means the SST product is produced from the local area coverage, which is the full resolution data stream downloaded on acquisition to a ground station within line of sight of the satellite. LAC is not available globally, but there is good provision of receiving stations to cover European coastal and shelf waters and much of the North Atlantic Ocean.

Table 4. Summary of satellite SST data products available over European seas

4.2.2 Combining data from different sources

It is one thing to decide in concept that the data from different types of SST sensors should be combined in order to benefit from their complementary sampling characteristics; it is another to implement a system in which this can be done without introducing more errors that result in a poorer assimilation performance than using a single SST data product from a single sensor. If each of the sensors measured precisely the same value of SST with the same accuracy then each data value could be used with equal weight, although the coarser spatial resolution of the microwave data would still have to be taken into account.

In practice, there are at least three factors in addition to their different spatial resolutions which cause the different data products to deliver different values of SST. These are:

- a) different accuracy, with errors in calibration and noise leading to a different bias and standard deviation when compared against an *in situ* “standard” of SST;
- b) the fact that different methods of measuring SST result in different values even when there are no measurement errors, because they sample different parts of the near surface thermal microstructure; and
- c) there are circumstances where the measured SST varies considerably throughout the day because of a strong diurnal variability signal.

Factor (a) is unavoidable when different sensor measurement techniques are being used. It is best treated by obtaining a confident knowledge of the errors (mean bias and standard deviation) associated with each measurement type. However, it is important when estimating the errors that factors (b) and (c) are also taken into account and do not create additional bias or variance. Factors (b) and (c) both relate to the physical behaviour of the upper layer of the ocean and are discussed in the next paragraph.

A particular problem that faces the use of SST measurements is that of the difference between precisely which part of the sea surface is being measured, as mentioned already in Section 3.3.4. Figure 8 identifies the difference between the skin SST which is measured by an infrared radiometer and the sub-skin SST a short distance below the surface (of order tenths of a millimetre). They are separated by the thermal skin layer where heat transport is restricted to molecular conductivity because of the suppression of turbulence close to the surface. The sub-skin is typically a few tenths of a degree warmer than the actual skin. Microwave radiometers measure the temperature at approximately the same depth as the sub-skin. Thus when microwave and infrared SST measurements are compared the thermal skin layer difference must be modelled and allowed for.

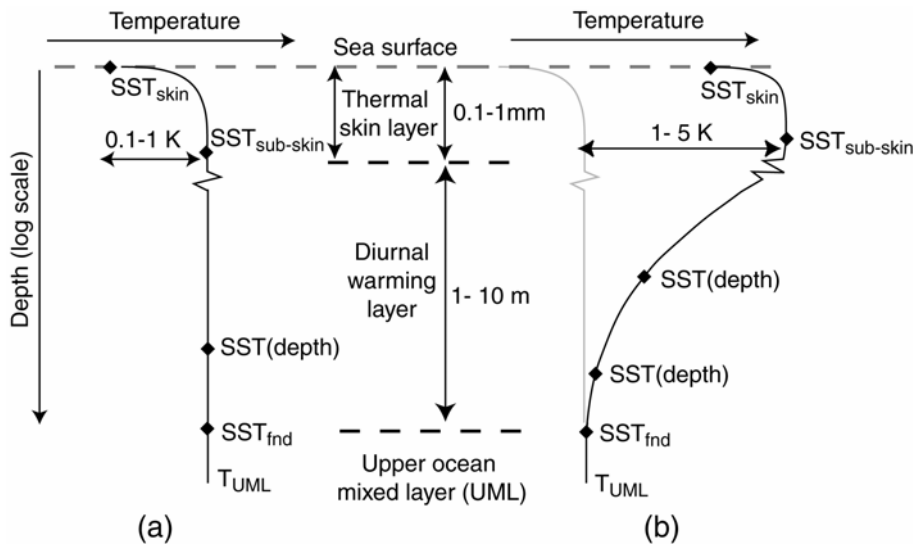


Figure 8. Schematic diagram showing characteristic temperature profiles at the sea surface for (a) night time conditions or daytime with moderate to strong winds and (b) daytime calm to light wind conditions and direct solar heating.

Both infra red and microwave measurements are different from the temperature sampled by an *in situ* sensor, normally used for calibration purposes. A thermometer in contact with surface sea water is typically mounted on the hull of a buoy or ship and located a distance of order 1 m below the surface. In circumstances of daytime cloud-free conditions and low wind the sun tends to heat up the water near the surface, inducing a thermal gradient in the upper metre or so. Consequently an *in situ* measurement of SST may be cooler than the satellite measurement. This diurnal thermocline develops to a maximum in the early afternoon and then reverts to a mixed layer of uniform temperature during the night. Thus the difference between the satellite measurement and an *in situ* measurement used to calibrate it can vary by up to several K through the day, depending on the surface solar irradiance and the wind history during the day. None of the SST data products listed in Table 4 take these factors into account in their processing. Consequently to use the data products as they are presented could lead to additional errors in the data being fed to the model, especially when they are combined, since the different response of each type of data to these factors introduces a spurious variability. This is the underlying problem which led to the development of the GHRSSST-PP project.

4.2.3 The GHRSSST data processing model

The GHRSSST-PP project has approached the problems identified in the previous section by adopting a particular model of the thermal structure of the near surface of the ocean and with it defining clear terminology that is intended to avoid confusion and misunderstanding in the use of the loose term “SST” which can have several meanings. A distinction is made between skin and sub-skin SST as outlined in 4.2.2, and a new term, the “foundation SST” or SST_{fnd} is used to describe the temperature on which the diurnal warming (if any) is built each day. It is most clearly specified as the temperature of the well mixed layer found just below the skin layer at dawn, when any diurnal thermocline structure from the previous day has collapsed. At this time of day it is equivalent to the subskin SST. The SST_{fnd} is defined on a daily basis. It also corresponds closely to the temperature of the upper layer of the ocean most commonly represented in numerical ocean circulation models that do not attempt to represent diurnal warming. The use of this name is preferred instead of the term “bulk” SST. The latter is very imprecise because it tends to be used also for any *in situ* measurement made by a thermometer in contact with the water (as distinct from a radiometric measurement which observes the skin SST) which may or may not be influenced by the diurnal thermocline, depending on the depth of the thermometer and the character of a particular day’s diurnal variability.

A key aspect of the GHRSSST processing model is that satellite measurements are recognised to be either skin or subskin temperatures, while it is assumed that the temperature normally required by models is the SST_{fnd} . The relationships between each of the different SST quantities are parameterised in terms of the controlling air-sea interaction quantities, particularly the wind speed and the solar irradiance, and these are expected to vary during the day. Note that the difference between skin and subskin (the thermal skin deviation), and between subskin and foundation (the diurnal warming) are different and controlled by largely independent processes. It is envisaged that when SST values are needed to high accuracy for ingestion into a numerical ocean model, adjustments will be applied to convert the satellite measurement of skin or subskin SST into the appropriate value of SST_{fnd} . However, there are circumstances where a model may need to use the skin temperature, for example when estimating air-sea fluxes, and in this case the GHRSSST-PP processing model specifies how conversion can be made from SST_{fnd} to SST_{skin} .

The approach outlined in the previous two paragraphs provides a framework in which problems (b) and (c) from 4.2.2 are handled. It is also intended that errors caused by (b) and (c) should be isolated from the more general biases and errors of (a). The latter need to be provided along with the basic temperature data to allow the model assimilation system to weigh the importance to be attached to a particular SST ingest. Therefore

GHRSSST-PP has specified a core SST product which consists of the same SST data as received from the original processing agency (e.g. one of the data products listed in Table 4) with the addition of:

- i. a confidence value associated with the probability of the data being corrupted by such things as cloud cover (IR only), high winds (m/w only), diurnal warming and proximity to land;
- ii. single sensor error statistics (SSES) defining the bias and standard deviation applicable to that particular sensor depending on the confidence flag; and
- iii. sufficient information to be able to calculate the parameterized values of the thermal skin deviation and diurnal warming at the precise time of the satellite sample (allowing conversion to SST_{fnd}).

Note that for this basic product there is no intention of resampling or regriding the data specified in Table 5, which are typically Level 2 image datasets (presented in the sensor co-ordinates). Hence it is referred to as the GHRSSST-PP L2P product (level 2 pre-processed). Neither is there any merging of data from different sources. It is assumed that the model assimilation scheme can handle the native grids of the inputs, and any differences in bias between them, better than any pre-processing or blending which risks introducing unnecessary additional errors. However, the addition of (iii) allows the assimilation system to make the conversion to whatever definition of SST is appropriate for the model, while the provision of (i) and (ii) allows the influence of data assimilated into a model to be weighted according to its quality. Note that the SSES in (ii) should be calculated on the basis of matching against independent validation measurements of temperature, after making the appropriate correction to adjust between skin, subskin or foundation SST so that comparison is made between like quantities. Thus the bias and standard deviation should no longer contain an element caused by inappropriately comparing unlike quantities (although they may contain a contribution from errors in the method used to perform the conversions).

There are four main product types proposed by the GHRSSST-PP processing model:

- The L2P product described in the previous two paragraphs, intended as the primary source of data for assimilation into numerical ocean forecasting models, and therefore required in near-real time.
- A match-up data base (MDB) that pairs spatially and temporally coincident values of SST independently measured *in situ* and by satellite.
- Diagnostic data sets (DDS) will be produced for a number of small regions chosen to represent different ocean and atmosphere conditions around the world.
- An analysed SST product at level 4 that is a blend of all the available SST data, each converted to SST_{fnd} and then used in an optimal

interpolation (OI), or other analysis technique, to create the best daily fields of SST_{ind}, without any cloud gaps.

The processing models required to generate these products are fully defined in the GHRSSST Data-processing System document, the current version of which is GDS v1.5, available online from <http://www.ghrsst-pp.org>. The model is an active document, still being refined in the light of working experience.

4.3 Putting the GHRSSST processing model into action

GHRSSST-PP has evolved rapidly to meet the perceived need for a new class of merged SST products. After four Workshops the Science Team produced an implementation plan that was approved by GODAE, its parent body. GHRSSST-PP is now established through the creation at the UK Met. Office of an International Project Office sponsored by the European Space Agency (ESA). While this provides leadership and co-ordination, the development comes from work at a regional level, through the GHRSSST-PP regional data assembly centres (RDAC)s. One of these already existed through a Japanese SST programme for the Asian Pacific area. The function of a European RDAC is now being fulfilled by a project within the ESA's Data Utilisation Envelope (DUE) Programme called "Medspiration". The Multi-sensor Improved SST Project (MISST), has been established by the National Ocean Partnership Programme in USA to support the function of an American RDAC. When fully implemented GHRSSST-PP should make a considerable impact on the quality of SST data available for operational oceanography worldwide.

As the European RDAC for GHRSSST-PP the Medspiration project, which commenced in January 2004, contributes to the development of an operational oceanography system within the European Union's Global Monitoring for Environment and Security (GMES) programme. The core user need identified for Medspiration was for SST products at high resolution (~10 km) over the Atlantic Ocean and adjoining Seas, which combine the best of all the SST data products already available from individual sensors. The desired temporal resolution is 6 hrs. The required accuracy of SST data is to be better than 0.4 K, with a goal of 0.1 K. Since Medspiration will use the SST sources in Table 4, which are already supplied by various agencies, it will always depend on the quality of the data being ingested.

However, it will for the first time provide European operational users not only with a near-real time single point access to data from all the different SST sources but also with robust error and confidence statistics attached to the SST products. This capacity to assign quality values to all the SST data sources being used, and to any future SST products that may be generated, is a fundamental requirement of GHRSSST-PP. It is needed in order to

facilitate the assimilation of SST products into operational ocean models and forecasting systems.

Medspiration will produce four types of data product. These are elaborated as follows:

Level 2 pre-processed SST data: ESA's Medspiration project will generate L2P data, as defined in Section 4.2.3, within a few hours of the input L2 SST products being served by their respective agencies. The area coverage is the whole Atlantic Ocean and adjacent seas. In the User Requirements Document (URD) produced by GHRSSST-PP the EurDAC area is defined as encompassing the area 70°S to 90°N (to the ice limit) and from 100°W to 45°E (to include the adjacent seas but excluding any part of the Pacific Ocean).

Level 4 gridded, interpolated SST data product: An L4 product will be produced for the Mediterranean Sea, consisting at each grid cell of a single daily value of SST_{find} produced by the optimal interpolation process, plus an estimate of the expected diurnal stratification and skin effects every two hours. Error estimates will also be provided for every temperature estimate. The ultra-high resolution (UHR) grid for this product is 2×2 km. Delivery is due by noon on the day following that to which it refers.

The software for generating the L4 product is designed with sufficient flexibility to allow the parameters in the OI scheme to be changed. Similarly the form of the model defining the differences between skin, subskin and foundation SST can be adjusted in future following operational experience and analysis of the resulting L4 products. The main purpose of the L4 product in GHRSSST is to meet the demand from general users of SST for a product which best combines all of the available primary sources of SST from different sensors.

A match-up data base (MDB) will be produced, which assembles matched pairs of all available in situ measurements of SST that are coincident with satellite measurements from the ingested L2 SST data within the Medspiration domain. It is most convenient to create the MDB in near-real time when the L2P data have just been produced. Medspiration will make use of the French Coriolis Data Centre used to assemble in situ data although, the difficulty of timely delivery of some in situ SST samples is likely to delay the MDB creation by up to a week after real time.

The MDB will be analysed regularly to allow GHRSSST to update frequently (say once per week or every few weeks) the sensor specific error statistics (SSES) attached to the L2P product, needed for assimilation and also in the OI procedure. It is also important that a broad spatial coverage is achieved by the MDB so that the SSES are properly spatially representative and can also be stratified by confidence value.

A diagnostic data set (DDS) of SST observations will be compiled for the Medspiration L2P product area by extracting $1/100^\circ \times 1/100^\circ$ gridded sub scenes for a set of predefined small areas (typically $2^\circ \times 2^\circ$ in extent) from

every L2P and L4 product produced by the Medspiration processor. Each product will be resampled (nearest neighbour) onto a common grid to facilitate analysis. Where possible the DDS sites have been chosen to coincide with known locations of regular in situ measurements (e.g. PIRATA buoys, Ferry-Box routes).

Within Medspiration the DDS will allow close comparison to be made between the different input streams of SST and with the L4 output. One objective is to provide a prompt alert should a particular sensor start to deviate seriously from the others. Another is to facilitate the research needed to test and improve the data merging methods, diurnal variability parameterisations and OI configuration used both in Medspiration and more widely in GHRSSST-PP.

4.4 Lessons to be learned from the GHRSSST-PP and Medspiration approach

Although still in the development stage and not scheduled to commence a demonstration of operational capability before early 2005, GHRSSST-PP and its European contributor Medspiration have been singled out for this case study because they provide a pathfinding example of what can be achieved when data providers and the remote sensing scientists working with them turn their attention to the needs of users, and in this case the requirements of the ocean modelling community for SST data to be assimilated into ocean forecasting models. It is worth noting that, although GHRSSST-PP has been driven largely by the science team of satellite oceanographers and data providers, it was spawned in the first place by the modellers in GODAE and has at all stages interacted strongly with its intended users in the ocean modelling community, who have attended the science team meetings and endorsed the implementation plan and the data processing model. This was recognised by ESA when they decided to initiate the Medspiration Project within their DUE Programme. The Medspiration project is thus not so much a science development project as primarily a software contract to develop a system to meet the needs identified in the Medspiration User Requirements Document.

Stepping back from the details which are specific to SST measurements, there are more general lessons to be learned about the preparation of satellite data in order to make it more useful to the modelling community, as follows.

1. Attempts should be made to widen the spatial and temporal coverage of remote sensing by using data from different sources, especially when they offer complementarity of sampling. Ideally use should be made of the products being produced by agencies already, without changing them apart from adding error statistics and confidence flags. This implies an active partnership with the data supplying agencies.

2. The different characteristics of data from different sources needs to be recognised. The goal should be to harmonise them, accommodating the differences in a suitable physical model that parameterises them in terms of measurable and routinely available quantities.
3. Merging of data from different sources is not necessarily the best approach. Dialogue with the model assimilation specialists is essential before decisions are made about this.
4. If data are to be used for assimilation it is essential to provide error statistics and quality flags in near real time attached to the primary data. The error statistics must be based on independent measurements of the quantities actually represented in the data.
5. The concept of creating a match-up database appears to be a very useful approach to achieving validation by regularly updated error statistics for each sensor and data source. To be useful it needs to be populated in near-real time by matching satellite and *in situ* data pairs. However, care must be taken not to utilise data that is already being used as a means of calibration or fine tuning of processing algorithms by the agency responsible for the primary processing.
6. Diagnostic data sets, which assemble all the data available from different sources resampled to a common grid, provide a valuable resource for evaluation of the products. They will provide the ground on which to base research for further improvements.

Collaboration is essential between all the players concerned. Handled properly, this approach should be welcomed by the data producers as a means for making their products more useful, and also because rapid feedback from the MDB and DDS provides an external quality control. The potential users of SST in the modelling community find a group of scientists within GHRSSST-PP ready to work with them. Within this partnership the modellers should be able to use the data successfully without themselves needing to become experts in all aspects of the remote sensing methodology. Finally the scientists are able to contribute more effectively to the application of their work, which is not only professionally stimulating but ultimately enhances the profile of this field of research and improves the prospects for funding of further work.

5. Conclusion

This chapter has offered a brief introduction to ocean remote sensing and especially those methods which make measurements of parameters such as SSH, SST and colour that can usefully contribute to operational monitoring and forecasting of the ocean. There is considerable potential to enhance the usefulness of satellite ocean data by assimilating them in near-real time into

ocean models. Given recent advances in both numerical ocean modelling and satellite observing systems, it is expected that fully operational ocean forecasting systems will be in place within a few years. In future it is likely that oceanographers will turn to operational models, supported by a global ocean observing network of satellite and *in situ* sensors, to obtain the best knowledge of the ocean state at any time or place, in much the same way as meteorologists rely today on the analysis delivered by atmospheric numerical weather prediction models.

Further research and development are needed before this can be achieved. There is scope to refine the remote sensing methods described above, not only to improve the accuracy of measurements but also to specify the errors more confidently, which is important if they are to be assimilated into ocean models. Ways should be found to harmonise the data provided by different ocean colour sensors, comparable to what the GHRSSST project is doing for SST data products. A secure future for operational ocean forecasting systems also depends on planning now for continuity of appropriate sensors in space and needs commitment by funding agencies to the long term support of ocean monitoring satellites and buoy/drifter programmes which this implies. Such a commitment must be justified by sensitivity studies that clearly demonstrate the impact which the assimilation of particular ocean observations makes to the forecasting / nowcasting skill of ocean models. We can no longer expect new ocean monitoring satellites to be provided automatically as part of national or international space technology programmes. Alternative funding routes must be established so that ocean monitoring satellites can in future be commissioned by their users. It is therefore vital to spell out the benefits of large scale ocean observing and forecasting systems (e.g. Johannessen *et al.* 2003) so that society at large and especially those who use the sea will appreciate their potential benefits.

References

- Barton, I.J. (1995) Satellite-derived sea surface temperatures: Current status. *J. Geophys. Res.*, **100**: 8777-8790.
- Challenor P. G., Cipollini, P., Cromwell, D.D., Hill, K.L., Quartly, G.D., and Robinson, I.S. (2004) Global characteristics of Rossby wave propagation from multiple satellite datasets", *International Journal of Remote Sensing*, **25**(7-8): 1297-1302.
- Chapron, B., Johnsen, H. and Garello, R. (2001) Wave and wind retrieval from SAR images of the ocean. *Ann. Télécommun.*, **56**(11-12): 682-699.
- Chelton D.B., Wentz, F.J., Gentemann, C.L., De Szoeke, R.A. and Schlax, M.G. (2000) Satellite microwave SST observations of transequatorial tropical instability waves. *Geophys. Res. Lett.*, **27**: 1239-1242
- Chelton, D. B., Ries, J. C., Haines, B. J., Fu, L.-L. and Callahan, P. S. (2001) Satellite Altimetry. In: Fu, L.-L. and Cazenave, A. (eds) *Satellite Altimetry and Earth Sciences*, pp. 1-131. Academic Press, San Diego.

- Cotton, P. D. and Carter, D. J. T. (1994) Cross calibration of TOPEX ERS-1 and Geosat wave heights. *J. Geophys. Res.*, **99**: 25025-25033.
- Donlon, C. J., Gentemann, C. and Wentz, F. (2001) Measuring surface temperature with microwave sensors, *Backscatter*, **12**(2): 37-39.
- Edwards, T., Browning, R., Delderfield, J., Lee, D. J., Lidiard, K. A., Milborrow, R. S., McPherson, P. H., Peskett, S. C., Toplis, G. M., Taylor, H. S., Mason, I., Mason, G., Smith, A. and Stringer S. (1990) The Along Track Scanning Radiometer measurement of sea-surface temperature from ERS-1. *J. British Interplanetary Soc.* **43**: 160-180.
- Gower, J. F. R. (1996) Intercalibration of wave and winds data from TOPEX/Poseidon and moored buoys off the west coast of Canada. *J. Geophys. Res.*, **101**, 3817-3829.
- Johannessen, J.A., Ian Robinson, Kostas Nittis (2003) MERSEA strand 1, In: H. Dahlin, N.C. Flemming, K. Nittis, S.E. Petersson (eds.) *Building the European Capacity in Operational Oceanography, Proceedings of the Third International Conference on EuroGOOS, 3-6 December 2002, Athens, Greece*, Elsevier Oceanography Series, No. 69, 714 pp., ISBN 0-444-51550-X.
- Kidwell, K. (1991) *NOAA Polar Orbiter User's Guide*. NCDC/NESDIS, National Climatic Data Center, Washington, D.C.
- Le Provost, C. (2001) Ocean Tides,. In: Fu, L.-L. and Cazenave, A. (eds) *Satellite Altimetry and Earth Sciences*, pp. 267-303. Academic Press, San Diego.
- Kilpatrick, K.A., Podesta, G. P. and Evans, R. H. (2001) Overview of the NOAA/NASA Pathfinder algorithm for sea surface temperature and associated matchup database. *J. Geophys. Res.*, **106**: 9179-9198.
- McClain E. P., Pichel, W. G. and Walton, C. C. (1985) Comparative performance of AVHRR based multichannel sea surface temperatures, *J. Geophys. Res.*, **90**: 11587-11601.
- Merchant C.J., Harris, A.R., Murray, M.J. and Zavody, A.M. (1999) Toward the elimination of bias in satellite retrievals of sea surface temperature 1. Theory, modeling and interalgorithm comparison, *J. Geophys. Res.*, **104**(C10): 23565-23578.
- Murray, M.J. (1995) *Sea surface temperatures from ATSR (August 1991 to July 1995)*, (CD-ROM), Rutherford Appleton Lab., Chilton, England.
- Podesta, G.P., Sheno, S., Brown, J.W., and Evans, R.H. (1995) *AVHRR Pathfinder Oceans Matchup Database 1985-1993 (Version 18)*, draft technical report of the University of Miami Rosenstiel School of Marine and Atmospheric Science, June 8, 33pp.
- Reynolds, R.W. (1993) Impact of Mt. Pinatubo aerosols on satellite-derived sea surface temperatures, *J. Climate*, **6**: 768-774.
- Reynolds, R. W. and Smith, T. S. (1994) Improved global sea surface temperature analyses, *J. Climate*, **7**: 929-948.
- Robinson, I. S. (2004) *Measuring the Oceans from Space: The principles and methods of satellite oceanography*, Springer-Praxis, Chichester and Heidelberg, 670 pp.
- Robinson, I.S. and Cromwell, D.D. (2003) *Observational Requirements for inputs to European Ocean Forecasting System Models*, Report D 3.1 for the E.U. Framework 5 Project MERSEA Strand-1. Southampton Oceanography Centre, Southampton, U.K., 57 pp.
- Robinson, I. S. and Donlon, C. J. (2003) Global measurement of sea surface temperature from Space: some new perspectives. *Global Atm. Ocean System*, **9**(1-2): 19-37.
- Tapley, B. D. and fourteen co-authors (1994) Precision orbit determination for TOPEX/Poseidon. *J. Geophys. Res.*, **99**: 24383-24404.
- Vasquez, J., Perry, K. and Kilpatrick, K. (1998) *NOAA/NASA AVHRR Oceans Pathfinder Sea Surface Temperature Data Set; User's Reference Manual Version 4.0*. JPL Publication D-14070.
- Walton, C. C., Pichel, W.G., Sapper, J. F. and May, D. A. (1998) The Development and Operational Application of Nonlinear Algorithms for the Measurement of Sea Surface

- Temperatures with the NOAA Polar-Orbiting Environmental Satellites., *J. Geophys. Res.*, **103**: (C12) 27999-28012.
- Wentz, F. J. and Meissner, T. (2000) *AMSR Ocean Algorithm (Version 2)*, Algorithm Theoretical Basis Document (ATBD), Remote Sensing Systems, Santa Rosa, CA, Revised edition, November 2, 2000.
- Zavody, A.M., Mutlow, C.T. and Llewellyn-Jones, D.T. (1995) A radiative transfer model for SST retrieval for the ATSR, *J. Geophys. Res.*, **100**: 937-952.